

Article

New Titanium(IV)-Alkoxide Complexes Bearing Bidentate OO Ligand with the Camphyl Linker as Catalysts for High-Temperature Ethylene Polymerization and Ethylene/1-Octene Copolymerization

Vladislav A. Tuskaev^{1,2,*}, Svetlana Ch. Gagieva¹, Dmitrii A. Kurmaev¹, Yulia V. Nelyubina², Petr V. Primakov^{1,3}, Maria D. Evseeva¹, Evgenii K. Golubev^{2,4}, Mikhail I. Buzin², Galina G. Nikiforova², Pavel B. Dzhevakov¹, Viktor I. Privalov⁵, Kasim F. Magomedov¹ and Boris M. Bulychev^{1,*}

¹ Department of Chemistry, M. V. Lomonosov Moscow State University, 1 Leninskie Gory, 119992 Moscow, Russia

² A. N. Nesmeyanov Institute of Organoelement Compounds, Russian Academy of Sciences, Vavilova St. 28, 119991 Moscow, Russia

³ Department of Chemistry, Mendeleev University of Chemical Technology of Russia, Miusskaya pl. 9, 125047 Moscow, Russia

⁴ Enikolopov Institute of Synthetic Polymer Materials, Russian Academy of Sciences, Profsoyuznaya Str. 70, 117393 Moscow, Russia

⁵ Kurnakov Institute of General and Inorganic Chemistry, Russian Academy of Sciences, 31 Leninsky Prospect, 119991 Moscow, Russia

* Correspondence: tuskaev@tech.chem.msu.ru (V.A.T.); bmbulychev@gmail.com (B.M.B.)



Citation: Tuskaev, V.A.; Gagieva, S.C.; Kurmaev, D.A.; Nelyubina, Y.V.; Primakov, P.V.; Evseeva, M.D.; Golubev, E.K.; Buzin, M.I.; Nikiforova, G.G.; Dzhevakov, P.B.; et al. New Titanium(IV)-Alkoxide Complexes Bearing Bidentate OO Ligand with the Camphyl Linker as Catalysts for High-Temperature Ethylene Polymerization and Ethylene/1-Octene Copolymerization. *Polymers* **2022**, *14*, 4735. <https://doi.org/10.3390/polym14214735>

Academic Editors: Chen-I Yang, Jean-François Carpentier and Binyuan Liu

Received: 5 September 2022

Accepted: 31 October 2022

Published: 4 November 2022

Publisher's Note: MDPI stays neutral with regard to jurisdictional claims in published maps and institutional affiliations.



Copyright: © 2022 by the authors. Licensee MDPI, Basel, Switzerland. This article is an open access article distributed under the terms and conditions of the Creative Commons Attribution (CC BY) license (<https://creativecommons.org/licenses/by/4.0/>).

Abstract: In order to increase the thermal stability of olefin polymerization precatalysts, new titanium(IV) complexes with diolate ligands differing in the degree of steric hindrances were synthesized from readily available precursor (\pm)camphor. The structures of the complexes **1–2** were established by X-ray diffraction. Complexes **1–4** in the presence of an activator $\{Et_nAlCl_{3-n} + Bu_2Mg\}$ catalyzed the synthesis of UHMWPE with an M_v up to 10 million and a productivity of up to 3300 kg/mol_{Ti}·atm·h. The obtained polymers are obviously characterized by a low density of macromolecular entanglement, which makes it possible to use the solid-phase method for their processing. The mechanical characteristics of the oriented UHMWPE films had a breaking strength up to 2.7 GPa and an elastic modulus of up to 151 GPa. The precatalysts **1–4** were also active in ethylene/1-octene copolymerization. The comonomer content was in the range of 1.4–4.6 mol%. The use of a rigid linker and an increase in the steric load of the diolate complexes ensured the thermal stability of the catalytic system in the range of 50–70 °C.

Keywords: Ti(IV) complexes; OO-ligand; thermal stability; ultra-high molecular weight polyethylene; polyolefin elastomers

1. Introduction

The development of catalysts for the (co)polymerization of olefins based on transition metal complexes is one of the most advanced areas of modern organometallic chemistry [1–4]. However, research in this field will undoubtedly continue due to the constant need for new polymer materials. The value of new catalytic systems is determined not only by their productivity and the properties of the resulting polymers, but also by the technological parameters of the polymerization process, including the ability to operate in an acceptable temperature range.

Titanium-alkoxide complexes are perhaps one of the most accessible and inexpensive precatalysts. We know that titanium alkoxides in the presence of organoaluminum compounds are capable of catalyzing the polymerization of conjugated dienes [5–7] as well

as the oligomerization of ethylene. The best-known example is the alphabutol process, wherein the combination of $\text{Ti}(\text{OR})_4\text{-AlEt}_3$ is employed for the highly selective dimerization of ethylene to 1-butene [8].

At the same time, simple titanium alkoxides and more sophisticated alkoxo–titanium complexes have rarely been used for the polymerization of olefins. The ability to polymerize ethylene in the presence of activators traditional for the Ziegler–Natta catalysis is possessed by titanium–alkoxo complexes containing additional chlorine atoms or other donor atoms. Thus, the dichlorotitanium–alkoxide complex $[(\text{HOEt})\text{Ti}(\mu\text{-OEt})\text{OEt}(\text{Cl})_2]_2$ (Compound I, Chart 1), activated with MAO, catalyzes ethylene polymerization with an activity of up to 750 kg/mol h and propylene (up to 87 kg/mol h). This precatalyst unexpectedly displays a single-site behavior [9]. The alkoxo complexes II–III activated with MAO or AlEt_3 catalyze the formation of polyethylene along with a percentage of oligomers. The bischelated complex III appears to be the most active [10]. A titanium(IV)–dimeric complex IV stabilized by a benzoin derivative in the presence of MAO catalyzes ethylene polymerization with an activity up to 300 kg/mol·atm·h as well as the copolymerization of ethylene with norbornene. The catalytic systems are characterized by a long lifetime and the ability to produce high molecular weight linear PE and vinyl-type PNB [11]. One of the few examples of homoleptic and heteroleptic Ti(IV)–alkoxo complexes V–VI capable of polymerizing ethylene without the formation of oligomeric products is given in [12]. In the presence of $\text{Et}_3\text{Al}_2\text{Cl}_3$, these compounds catalyzed the formation of low molecular weight PE.

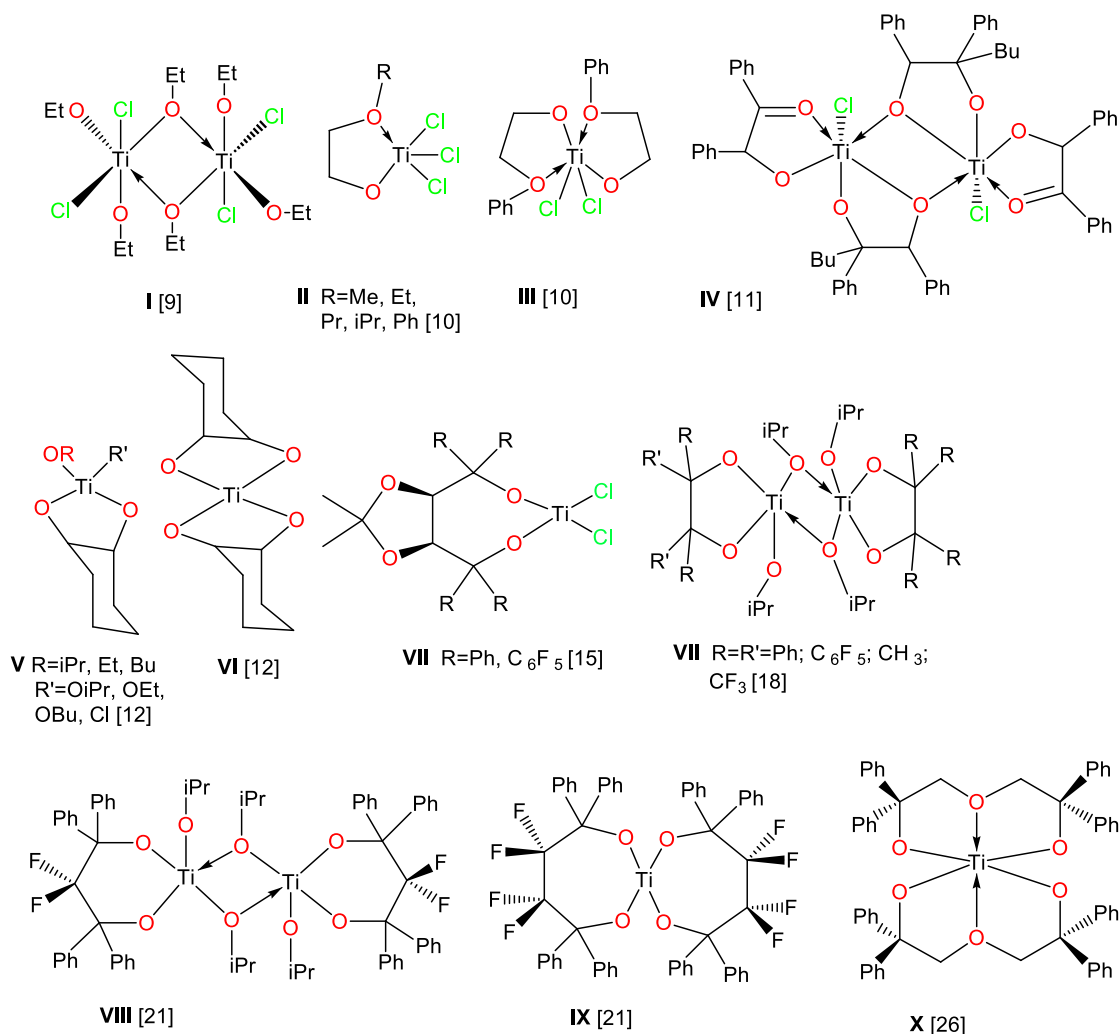


Chart 1. Examples of Ti(IV) complexes with diolate ligands used as olefin polymerization catalysts.

As was shown by Y. V. Kissin et al., the addition of the organomagnesium compound, e.g., Bu_2Mg to the mixture $\text{Ti}(\text{OiPr})_4\text{-Et}_2\text{AlCl}$ results in active, cheap, and affordable catalytic systems suitable for the polymerization of propylene [13] and the copolymerization of ethylene with higher olefins [14].

Previously, we reported on the ability of various titanium(IV)–diolate complexes VII–X [15–22], including those with additional heteroatoms [23–27] (Chart 1), to catalyze the (co)polymerization of ethylene in the presence of such Al/Mg activators. This group of postmetallocene precatalysts is poorly studied, which is most likely due to the specifics of their activation: in the presence of trialkylaluminum derivatives, alkylaluminum chlorides, or alkylaluminum oxanes (traditional activators in Ziegler–Natta catalysis), and the activity of these systems is low or does not manifest itself at all. However, when using the Al/Mg activators $\text{Alk}_n\text{AlCl}_{3-n} + \text{Bu}_2\text{Mg}$ (proposed by Yu. V. Kissin et al. [28,29]), their productivity in ethylene polymerization reached $4000 \text{ kg/mol}\cdot\text{atm}\cdot\text{h}$. It is important to note that, in most cases, these catalytic systems produce disentangled UHMWPE, which can be processed by the solid-phase method into high strength-oriented films and tapes, which are in high demand in various industries. In addition, such catalytic systems effectively catalyze the copolymerization of ethylene with higher olefins, and in some cases, even higher productivity is achieved up to 5 tons of copolymer /mol atm·h [20].

An essential point limiting the possibility of the industrial implementation of this group of catalysts is their low thermal stability. As a rule, the maximum productivity of such systems is achieved at a temperature of $30 \text{ }^\circ\text{C}$ [15–27]; an increase in the polymerization temperature to $50\text{--}80 \text{ }^\circ\text{C}$ is accompanied by deactivation and a significant reduction in the polymer's molecular weight. The aim of this work is the structural modification of the ligand environment of the metal, aimed at increasing the thermal stability of the considered precatalysts.

2. Experimental Section

All manipulations with air-sensitive materials were performed using standard Schlenk techniques. Argon and ethylene of a special purity grade (Linde gas) were dried by purging through Super Clean™ Gas Filters.

Toluene and nefras were distilled over Na/benzophenone ketyl, and the water content was periodically controlled by Karl Fischer coulometry by using a Methrom 756 KF apparatus. Diethylaluminum chloride, ethylaluminum sesquichloride, and di-*n*-butylmagnesium (Aldrich) were used without further purification. (\pm)-Camphorquinone was obtained by the method described in [30]. The preparation of the ligands L1 and L2 followed the procedure described in [31]; their properties corresponded to the literature data.

NMR spectra were recorded on a Bruker AMX-400 instrument (Mundelein, Illinois 60060 USA). Elemental analysis (C, H, Cl) was performed by the microanalytical laboratory at A. N. Nesmeyanov Institute of Organoelement Compounds on Carlo Erba-1106 and Carlo Erba-1108 instruments. The content of Ti was performed by X-ray fluorescence analysis on a VRA-30 device (Karl Zeiss, Germany).

$[\text{L}^1\text{Ti}(\text{OiPr})_2]_2$ (Complex 1). Ligand L1 (0.85 g, 5 mmol) and toluene (22 mL) were placed into a Schlenk tube equipped with a magnetic stirrer under an argon atmosphere, followed by the addition of $\text{Ti}(\text{OiPr})_4$ (1.42 g, 1.48 mL, and 5 mmol) at room temperature. The resulting suspension was heated until all solids dissolved. The next day, the formed crystals were collected by filtration and dried in vacuo. Yield 1.41 g (81.5%). Calculated (%) for $\text{C}_{32}\text{H}_{60}\text{O}_8\text{Ti}_2$ (668.55): C, 57.5; H, 9.0; O, 19.1; and Ti, 14.3. Found (%): C, 57.2; H, 8.6; and Ti, 14.0. ^1H NMR (400 MHz, CDCl_3), δ : 0.82 (s, 3H), 0.85 (s, 3H), 0.98 (s, 3H), 1.07 (s, 6H), 1.18 (s, 6H), 1.44 (s, 2H), 1.67 (s, 1H), 1.96 (s, 2H), 4.03 (d, $J = 20.2 \text{ Hz}$, 2H), and 4.32 (d, $J = 23.0 \text{ Hz}$, 2H). ^{13}C NMR (101 MHz, CDCl_3), δ : 88.18, 84.05, 77.35, 77.03, 76.71, 67.81, 64.45, 48.91, 47.87, 46.31, 31.90, 25.36, 24.30, 24.27, 23.65, 23.39, 23.25, 20.78, 20.41, and 10.67.

$[\text{L}^2\text{Ti}(\text{OiPr})_2]_2$ (Complex 2) was obtained by a similar method. Yield 1.34 g (74.2%). Calculated (%) for $\text{C}_{36}\text{H}_{68}\text{O}_8\text{Ti}_2$ (724.65): C, 59.7; H, 9.5; O, 17.7; and Ti, 13.2. Found (%): C, 59.4; H, 9.2; and Ti, 13.0. ^1H NMR (400 MHz, CDCl_3), δ : 0.87 (s, 3H), 0.89 (s, 3H), 0.96

(s, 3H), 1.09 (s, 6H), 1.12 (s, 3H), 1.20 (s, 3H), 1.23 (s, 3H), 1.65 (s, 3H), 1.94 (dd, $J = 29.4$, 4.9 Hz, 2H), 3.70 (s, 1H), 4.09 (m, 2H), and 4.36 (m, 2H). ^{13}C NMR (101 MHz, CDCl_3), δ : 80.39, 80.58, 77.23, 56.85, 53.20, 48.38, 30.99, 26.06, 25.62, 25.36, 24.36, 23.36, 23.23, 22.89, 21.53, 10.70, and 10.58.

L¹TiCl₂ 2iPrOH (Complex 3). In a 100 mL flame-dried Schlenk flask, ligand **L1** (0.85 g, 5 mmol) was dissolved in anhydrous toluene (20 mL). A solution of $\text{TiCl}_2(\text{OiPr})_2$ (1.185 g, 0.05 mmol) in toluene (20 mL) was added to the resulting solution under stirring in an argon atmosphere. The solution was stirred for 14 h at room temperature, and the precipitated complex was filtered off, washed with hexane (5 mL), and dried in a vacuum. The yield was 1.4 g (69%). Calculated (%) for $\text{C}_{16}\text{H}_{32}\text{Cl}_2\text{O}_4\text{Ti}$ (407.19): C, 47.2; H, 7.9; Cl, 17.4; O, 15.7; and Ti, 11.8. Found (%): C, 46.6; H, 7.6; Cl, 17.2; and Ti, 11.5. ^1H NMR (400 MHz, CDCl_3), δ : 0.88 (s, 3H), 0.92 (dd, $J = 38.4$, 11.9 Hz, 6H), 1.01 (s, 6H), 1.05 (s, 3H), 1.15 (s, 3H), 1.51 (s, 2H), 1.73 (d, $J = 4.8$ Hz, 1H), 2.04 (d, $J = 5.0$ Hz, 2H), 4.20 (s, 2H), and 4.39 (s, 2H). ^{13}C NMR (101 MHz, CDCl_3), δ : 87.99, 83.87, 67.62, 64.26, 48.72, 47.68, 46.12, 31.71, 25.17, 24.12, 24.09, 23.47, 23.06, 20.59, 20.22, and 10.48.

L²TiCl₂ 2iPrOH (Complex 4) was obtained by a similar method. Calculated (%) for $\text{C}_{18}\text{H}_{36}\text{Cl}_2\text{O}_4\text{Ti}$ (435.25): C, 49.7; H, 8.3; Cl, 16.3; O, 14.7; and Ti, 11.0. Found (%): C, 49.3; H, 8.0; Cl, 16.1; and Ti, 10.6. ^1H NMR (400 MHz, CDCl_3), δ : 0.89 (s, 3H), 0.92 (s, 3H), 0.96 (s, 6H), 1.20 (s, 6H), 1.32 (s, 3H), 0.89 (s, 3H), 1.92 (s, 3H), 1.68 (m, 2H, CH_2), 2.19 (m, 2H), 2.42 (s, 2H), 4.06 (m, 2H), and 4.78 (m, 1H).

2.1. X-ray Crystal Structure Determination

X-ray diffraction experiments were carried out at 100 K for **1** and at 240 K for **2** (below this temperature, the crystals of **2** cracked) with a Bruker D8 Quest diffractometer, using graphite monochromated Mo- $\text{K}\alpha$ radiation ($\lambda = 0.71073$ Å). Using Olex2 [32], the structures were solved with the ShelXT [33] structure solution program using Intrinsic Phasing and refined with the olex2.refine [34] refinement package using Least-Squares minimization against F^2 in anisotropic approximation for nonhydrogen atoms. Positions of hydrogen atoms were calculated, and they were refined in isotropic approximation within the riding model. Crystal data and structure refinement parameters for **1** and **2** are given in Table 1. CCDC 2189447 (for **1**) and 2189448 (for **2**) contain the supplementary crystallographic data for this paper.

Table 1. Ethylene polymerization by complexes **1–4** ^a.

Entry	Complex	Co Catalyst, [Al]/[Mg]	T °C	A, kg/mol·h·atm	M_v , 10 ⁶ Da	T_m , °C	Deg. of Crystal %	Bulk Density, g/cm ³
1	1	Et ₂ AlCl/Bu ₂ Mg	10	2114	5.85	140	79	0.063
2	1	Et ₃ Al ₂ Cl ₃ /Bu ₂ Mg	10	2629	5.97	140	55	0.080
3 ^d	1	Et ₃ Al ₂ Cl ₃ /Bu ₂ Mg	10	1600	7.68	143	55	0.056
4	1	EtAlCl ₂ /Bu ₂ Mg	10	2971	4.26	141	76	0.084
5 ^c	1	Et ₃ Al ₂ Cl ₃ /Bu ₂ Mg	10	457	8.51	144	88	0.080
6 ^{b,c}	1	Et ₃ Al ₂ Cl ₃ /Bu ₂ Mg	10	571	10.1	144	81	0.053
7	1	Et ₃ Al ₂ Cl ₃ /Bu ₂ Mg	30	2971	5.72	141	79	0.083
8	1	Et ₃ Al ₂ Cl ₃ /Bu ₂ Mg	50	3143	3.12	139	76	0.077
9	1	Et ₃ Al ₂ Cl ₃ /Bu ₂ Mg	70	2343	0.48	134	43	0.05
10	2	Et ₂ AlCl/Bu ₂ Mg	10	2874	4.01	143	59	0.071
11	2	Et ₃ Al ₂ Cl ₃ /Bu ₂ Mg	10	3069	4.8	143	55	0.092

Table 1. Cont.

Entry	Complex	Co Catalyst, [Al]/[Mg]	T °C	A, kg/mol·h·atm	M _v , 10 ⁶ Da	T _m , °C	Deg. of Crystal %	Bulk Density, g/cm ³
12	2	Et ₃ Al ₂ Cl ₃ /Bu ₂ Mg	30	2800	4.44	143	59	0.088
13	2	Et ₃ Al ₂ Cl ₃ /Bu ₂ Mg	50	2571	3.16	145	62	0.062
14	2	Et ₃ Al ₂ Cl ₃ /Bu ₂ Mg	70	1543	1.82	144	55	0.074
15	3	Et ₂ AlCl/Bu ₂ Mg	10	2743	2.91	141	41	0.066
16	3	Et ₃ Al ₂ Cl ₃ /Bu ₂ Mg	10	2971	6.81	144	78	0.077
17	3	EtAlCl ₂ /Bu ₂ Mg	10	3257	8.48	142	86	0.084
18	4	Et ₂ AlCl/Bu ₂ Mg	10	2777	2.63	141	66	0.078
19	4	Et ₃ Al ₂ Cl ₃ /Bu ₂ Mg	10	2874	6.65	143	65	0.086

^a Polymerizations were carried in 100 mL of toluene with 5×10^{-6} mol of precatalyst at a constant 0.7 atm of excessive ethylene pressure for 30 min and a molar ratio of Ti/Al/Mg = 1/300/100 (except for entries 4 and 17, where it was 1/200/100). ^b Preactivation of the complex within 24 h. ^c Polymerizations were carried out in 100 mL of nefras. ^d Pre-activation of the complex within 24 h.

2.2. Polymerization Experiments

The ethylene polymerization and ethylene/ α -olefine copolymerization techniques are described in detail in [21].

2.3. Polymer Characterization Methods

DSC was performed by a differential scanning calorimeter DSC-822e (Mettler-Toledo, Switzerland) at a heating rate of 10 °C/min in argon.

Viscosity average molecular weight of synthesized UHMWPE samples was calculated with the Mark–Houwink equation [35].

The technique for manufacturing-oriented films from UHMWPE nascent reactor powder and determining their mechanical characteristics is described in detail in [36].

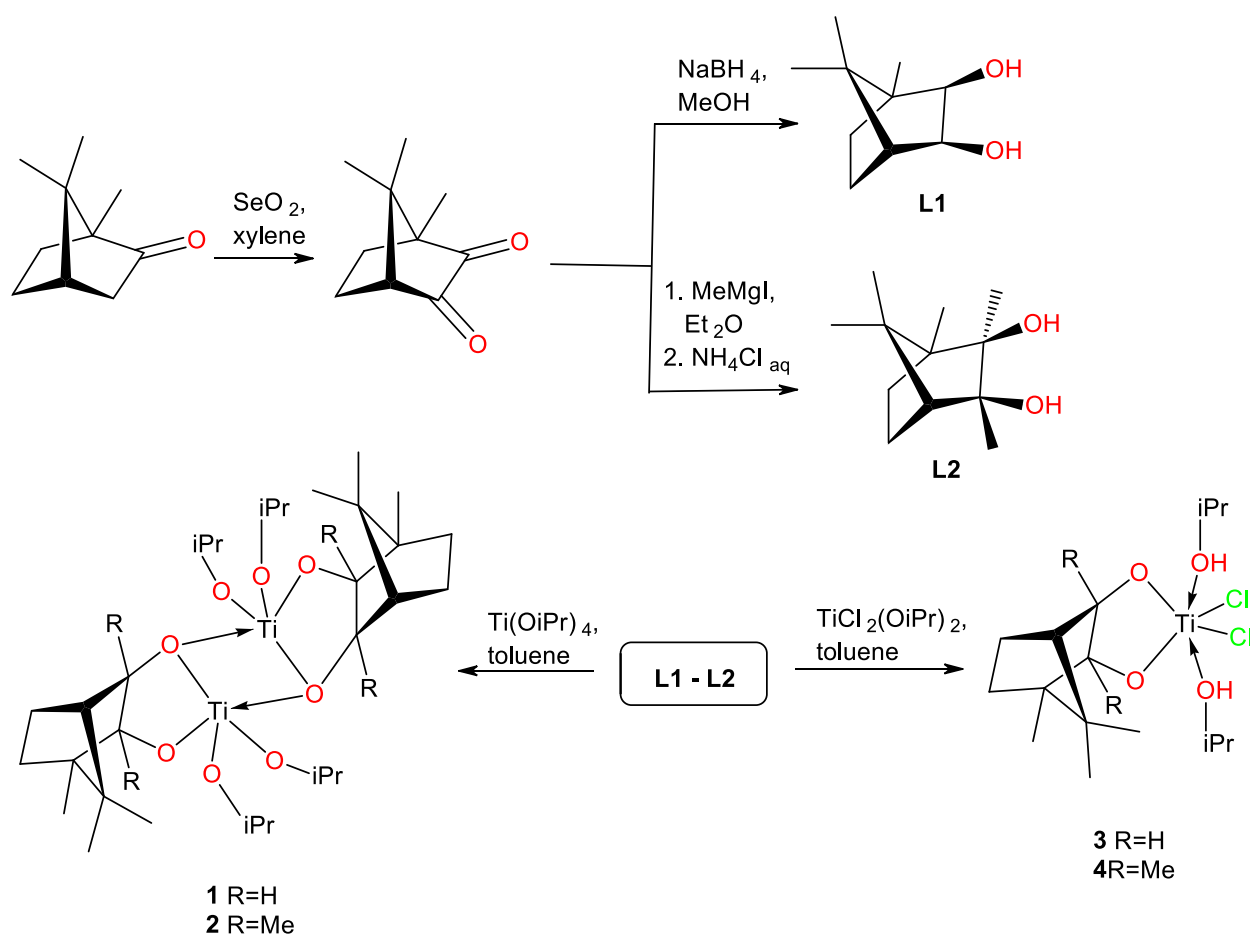
Scanning electron microscopy investigations of morphologies of nascent reactor powders were carried out with a high-resolution Tescan VEGA3 SEM operated at 5 kV. As-polymerized particles were carefully deposited on SEM stubs, and the samples were coated with gold by a sputtering technique.

¹³C NMR spectra of ethylene/octene-1 copolymers (~5 wt % solutions in dichlorobenzene) were recorded at 150 °C on a Bruker Avance-400 spectrometer at 101 MHz.

Gel permeation chromatographic (GPC) analysis of copolymers was carried out at 135 °C with a Waters GPCV-2000 chromatograph equipped with two columns (PLgel, 5 μ and Mixed-C, 3007.5 mm) and a refractometer. 1,2,4-Trichlorobenzene was used as a solvent; the elution rate was 1 mL min⁻¹. Molecular weights of polymers were determined using the universal calibration dependence relative to polystyrene standards with a narrow MW distribution: for polystyrene $K = 2.88 \times 10^{-4}$, $\alpha = 0.64$; for PE, and $K = 6.14 \times 10^{-4}$, $\alpha = 0.67$.

3. Results and Discussion

Commercially available (\pm) camphor was used as the initial compound for the synthesis of this group of ligands, the oxidation of which yielded camphoquinone (Scheme 1). Further, the reduction of camphoquinone with sodium borohydride or its interaction with methyl magnesium iodide yielded ligands L1–L2 (Scheme 1) differing in the steric load of hydroxyl groups.



Scheme 1. Synthesis of complexes 1–4.

Alkoxo–titanium(IV) complexes **1–2** were obtained by the reaction of the ligands **L1–L2** with $\text{Ti}(\text{OiPr})_4$ in a toluene solution. All compounds were isolated in 69–82% yields as air-sensitive powders, which are soluble in aromatic hydrocarbons. Titanium–dichloride complexes **3–4** were synthesized by direct interaction of the ligands **L1–L2** with one equivalent of $\text{TiCl}_2(\text{OiPr})_2$ in toluene. The compositions and structures of complexes **1–4** were confirmed by elemental analysis and ^1H and ^{13}C NMR spectroscopies. The integration of the NMR signals confirmed the presence of two isopropoxy groups per ligand unit in the reaction product. The structures of the complexes **1–2** were unambiguously established by X-ray diffraction study and are shown in Figure 1 along with the atomic numbering scheme. Experimental data for the X-ray diffraction studies of compounds and selected bond lengths and angles are given in Tables S1 and S2.

The complexes **1** and **2** crystallize in the triclinic space group P-1 with a half of the complex species being symmetry-independent; the appropriate symmetry element, the inversion center, is located in the geometric center of a Ti_2O_2 cycle. Each titanium(IV) ion coordinates two isopropoxy groups and two camphorquinone ligands that act both as a bridging ligand and a chelate ligand (Table 1). The resulting coordination polyhedron is a distorted square pyramid, as gauged by continuous symmetry measurements [37]. They measure how close the shape of the polyhedron is to a reference shape, such as an ideal square pyramid (SPY-5). The lower the value of an appropriate symmetry measurement, the better the fit is to a chosen polyhedron (Table S2).

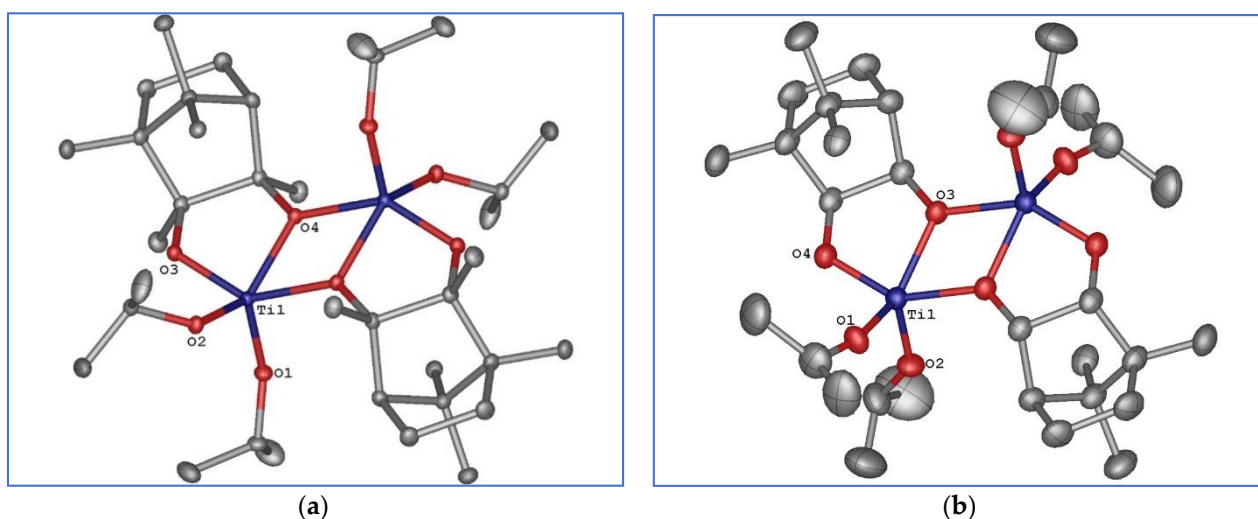


Figure 1. General view of the compounds **1** (a) and **2** (b) in representation of atoms via thermal ellipsoids at 30% probability level. Both molecules occupy the special positions, the inversion centers, as obtained by X-ray diffraction at 100 and 240 K. Hydrogen atoms are omitted for clarity. In both crystals, the complex occupies a special position, the inversion center, so only labels of symmetry-independent heteroatoms are given.

The catalytic activity of new titanium–diolate complexes **1–4** was studied in ethylene polymerization (Table 1). To activate precatalysts, binary activators {Et₂AlCl or Et₃Al₂Cl₃+Bu₂Mg} at a molar ratio of Al/Mg = 3/1 [28,29], were used. For the activator {EtAlCl₂+Bu₂Mg}, a molar ratio of Al/Mg = 2/1 was used since according to [21], it is precisely this ratio of the activator components that makes it possible to achieve the maximum productivity of diolate–titanium complexes.

For complex **1**, the effect of the nature of the organoaluminum compound (EtAlCl₂, Et₂AlCl, and Et₃Al₂Cl₃) contained in the Al/Mg activator on the productivity of catalytic systems and the properties of the resulting polymer were studied (entries 1, 2, and 4; Table 1). The maximum activity was shown by the system containing EtAlCl₂—a compound exhibiting the maximum Lewis acidity.

For the dichloride complex **3**, this pattern changes slightly: in a row Et₂AlCl, Et₃Al₂Cl₃ and EtAlCl₂ there is a consistent increase in both the productivity of the system and the molecular weight of polymers (entries 15–17, Table 1).

Comparing the effect of the nature of the organoaluminum component of the activator on the properties of the resulting polymer, it can be noted that for dichloride complexes **3–4**, the replacement of Et₂AlCl by Et₃Al₂Cl₃ led to a very significant increase in molecular weight (by 2.3–2.6 times (entries 15 vs. 16 and 18 vs. 19, Table 1). In the case of alkoxide complexes **1–2**, this effect also manifested itself, but to a much lesser extent (no more than 1.2 times, entries 1 vs. 2 and 10 vs. 11); a similar trend was seen previously [21,26].

Preactivation (holding the precatalyst with a small amount of activator in a Schlenk tube for 24 h) led to a significant drop in activity, from 2629 to 1600 kg/mol·h·atm, with a simultaneous significant increase in the molecular weight of the polymer (from 5.9 up to 7.7 × 10⁶ Da). The replacement of the aromatic solvent toluene with the aliphatic one nefras was accompanied by a very significant decrease in activity (from 2629 to 460 kg/mol·h·atm and an equally noticeable increase in M_v from 5.9 to 8.5 × 10⁶, and the use of preactivation technique in aliphatic solvent made it possible to increase this value to 10.1 × 10⁶ Da (entries 5 and 6, Table 1).

For the alkoxo complexes **1** and **2**, the influence of the polymerization temperature on the activity and on the molecular weights of the resulting polyethylene was studied (Figure 2). It was established that both complexes exhibited a sufficiently high thermal stability: for complex **1** with an increase in the polymerization temperature from 10 to

50 °C, the activity increased by 20%. At a temperature of 70 °C, the activity remained quite high at 2300 kg/mol_{Ti}·atm·h.

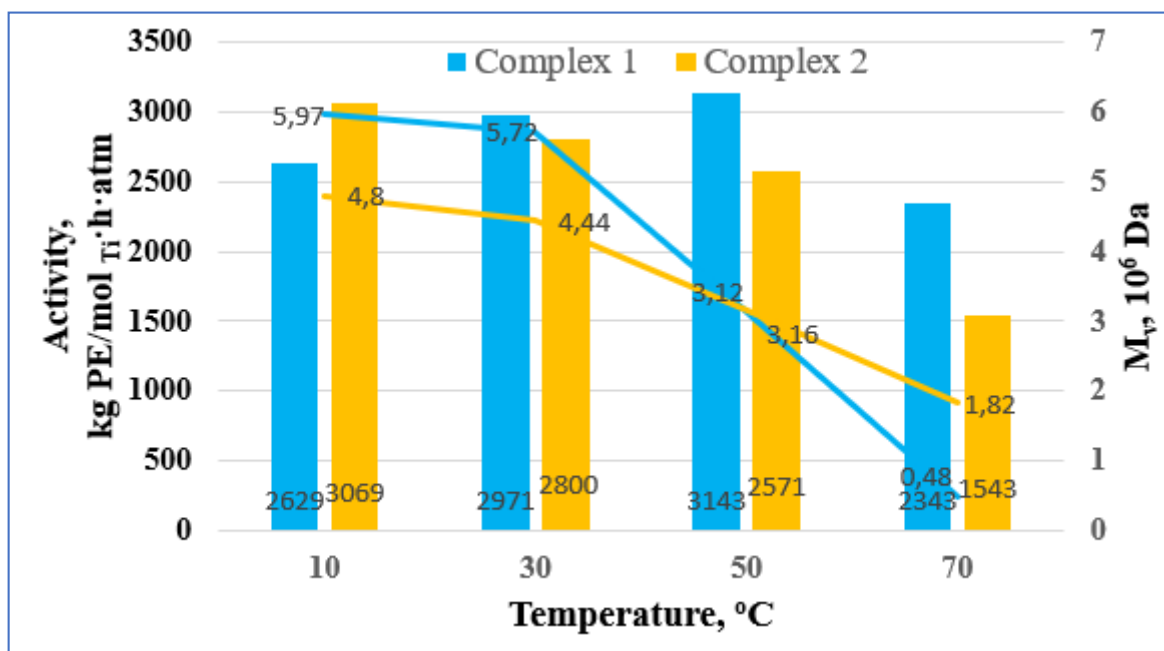


Figure 2. Influence of polymerization temperature on productivity of catalytic systems and polymer M_v .

Complex 2 with the sterically more hindered ligands behaved somewhat differently: the maximum activity (3100 kg/mol_{Ti}·atm·h.) appeared at 10 °C, and with an increase in the polymerization temperature, the activity consistently decreased to 1500 kg/mol_{Ti}·atm·h. at 70 °C.

With an increase in the polymerization temperature, the processes of polymer chain termination were accelerated, which is reflected in a significant decrease in the molecular weights of the polymer. However, the polymers obtained at 50 °C and even 70 °C (for complex 2) were ultra-high molecular weight polyethylenes. Thus, the process temperature allowed us to control the molecular weight of the resulting polymers.

The morphology and molecular weight are important characteristics of UHMWPE nascent reactor powder, which determine the efficiency of its processing into high modulus- and high strength-oriented materials. To examine the morphologies of these powders, scanning electron microscope (SEM) observations were performed (Figure 3). At a low magnification (Figure 3, top), the UHMWPE powder particles do not have a spherical shape, typical for the polymer obtained on classical Ti/Mg catalysts. The irregular shape and porous structure of the powder particles determine the low bulk density (0.05–0.088 g/cm³) of the obtained samples.

At high magnifications (Figure 3, bottom), the UHMWPE powder particles have a broccoli-like shape and differ in the number of fibrils connecting the globules.

The processing of the obtained UHMWPE reactor powders into high modulus-oriented films was carried out by preparing monolithic samples under pressure and shear deformation at an elevated temperature below the polymer melting point with a subsequent uniaxial drawing [36]. Mechanical tests were carried out for the samples oriented to the prefracture state, which varied for different samples (Table 2, Figure 4).

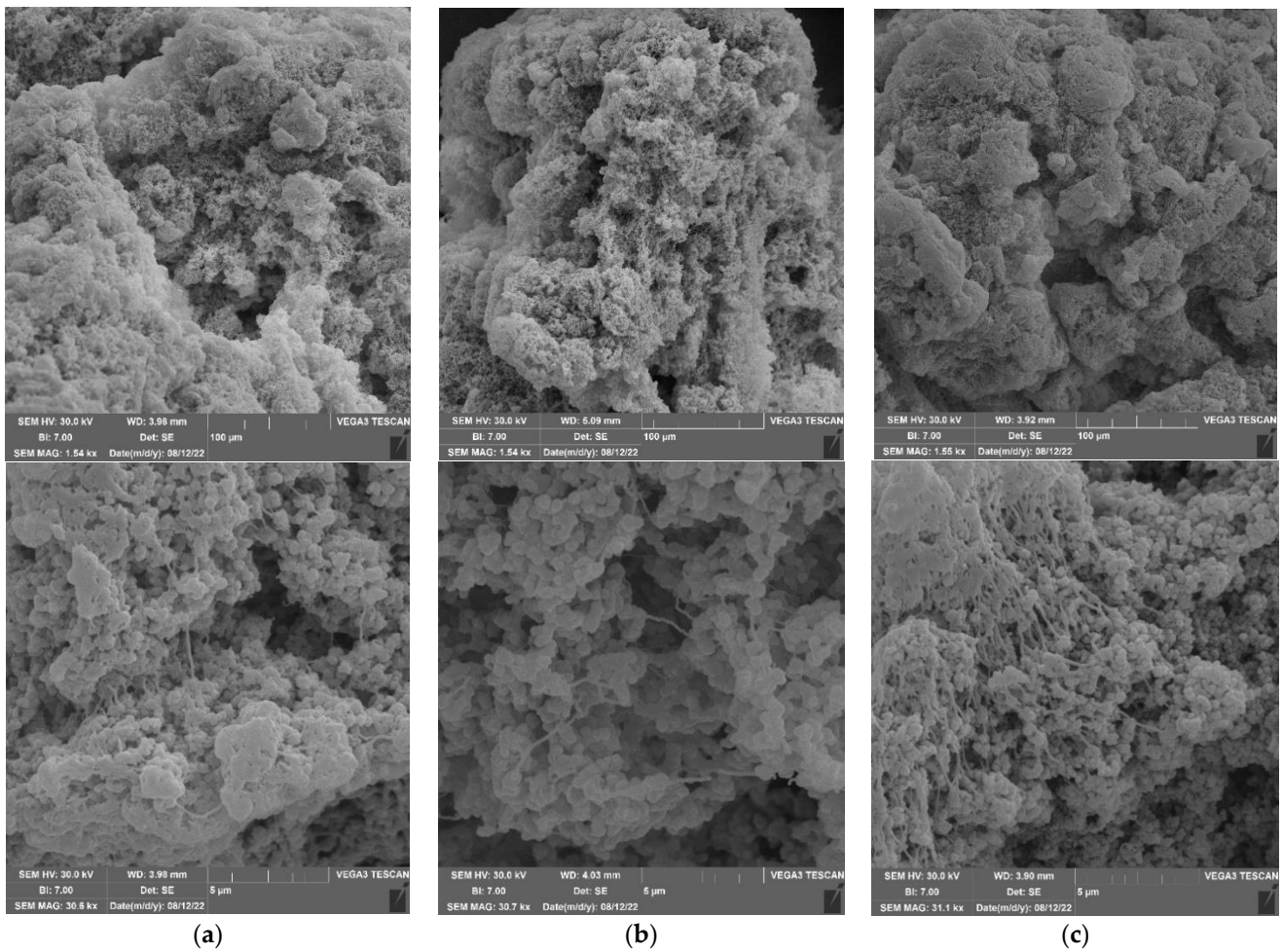


Figure 3. SEM images of the surface morphology of UHMWPE powders obtained with catalytic system 1/ $\text{Et}_2\text{AlCl}+\text{Bu}_2\text{Mg}$ ((a), entry 1); 1/ $\text{EtAlCl}_2+\text{Bu}_2\text{Mg}$ ((b), entry 4); and 1/ $\text{Et}_3\text{Al}_2\text{Cl}_3+\text{Bu}_2\text{Mg}$ ((c), entry 3) in nefras.

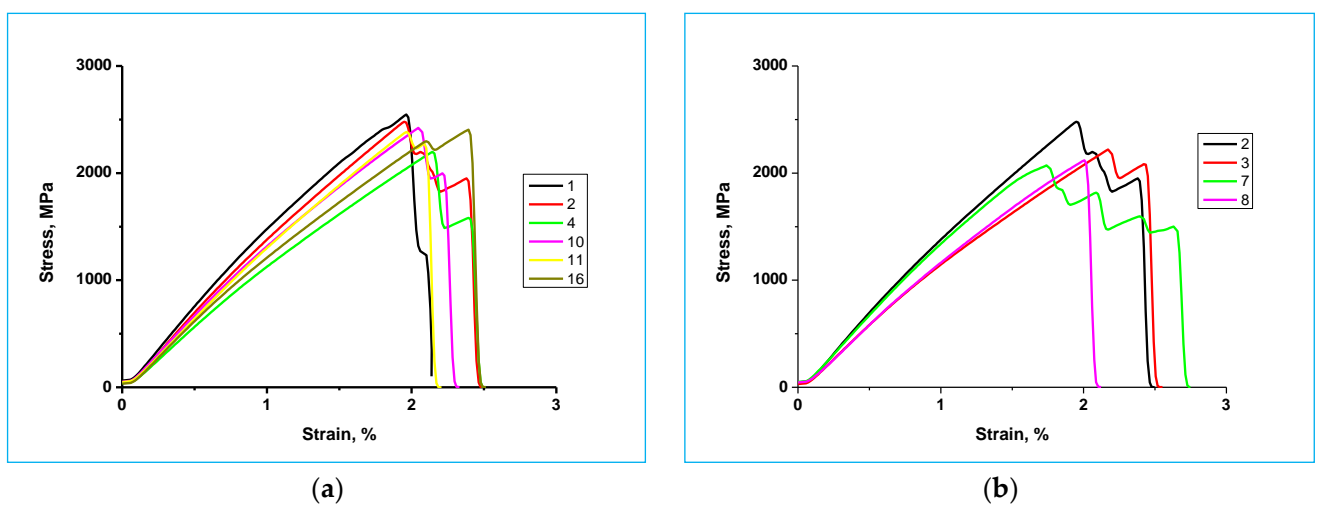


Figure 4. Stress–elongation curves for UHMWPE -orientated tapes. (a) entries 1,2,4,10,11, and 16; (b) entries 2,3,7, and 8 and Tables 1 and 2.

Table 2. Mechanical properties of UHMWPE-oriented film tapes ^a.

Entry	Catalytic System	Tensile Strength, σ , GPa	Average Tensile Modulus, E , GPa
1	1/Et ₂ AlCl+Bu ₂ Mg	2.3–2.7	147–151
2	1/Et ₃ Al ₂ Cl ₃ +Bu ₂ Mg	2.2–2.6	138–149
3 ^b	1/Et ₃ Al ₂ Cl ₃ +Bu ₂ Mg	1.7–2.4	114–137
4	1/EtAlCl ₂ +Bu ₂ Mg	1.5–2.6	119–137
7 ^c	1/Et ₃ Al ₂ Cl ₃ +Bu ₂ Mg	2.1–2.3	123–141
8 ^d	1/Et ₃ Al ₂ Cl ₃ +Bu ₂ Mg	1.7–2.2	111–135
10	2/EtAlCl ₂ +Bu ₂ Mg	2.1–2.7	128–136
11	2/Et ₃ Al ₂ Cl ₃ +Bu ₂ Mg	2.4–2.6	132–142
12 ^c	2/Et ₃ Al ₂ Cl ₃ +Bu ₂ Mg	1.8–2.5	112–149
13 ^d	2/Et ₃ Al ₂ Cl ₃ +Bu ₂ Mg	2.0–2.4	120–135
14 ^e	2/Et ₃ Al ₂ Cl ₃ +Bu ₂ Mg	1.6–2.0	108–123
15	3/EtAlCl ₂ +Bu ₂ Mg	1.9–2.4	116–129
16	3/Et ₃ Al ₂ Cl ₃ +Bu ₂ Mg	1.6–2.7	124–146
18	4/EtAlCl ₂ +Bu ₂ Mg	1.8–2.4	116–122
19	4/Et ₃ Al ₂ Cl ₃ +Bu ₂ Mg	2.0–2.5	132–139

^a Numbering corresponds to Table 1. ^b Preactivation of the complex within 24 h. ^c Polymerization was carried out at a temperature of 30 °C. ^d Polymerization was carried out at a temperature of 50 °C. ^e Polymerization was carried out at a temperature of 70 °C.

The UHMWPE nascent reactor powders obtained on bis-isopropoxo-titanium precatalysts **1** and **2** (entries 1,2,10, and 11) were processed into oriented films with approximately the same mechanical characteristics (Figure 4a). The nature of the organoaluminum compound (OAC) included in the Al/Mg activator did not significantly affect these parameters. The results obtained slightly exceeded those previously published for titanium complexes with diol ligands [17,18,21,25–27]; however, the reason may be not only the structure of the precatalysts, but also the polymerization temperature (in the cited works, polymerization was carried out at 30 °C). For comparison, the modulus value for commercially available gel-spun UHMWPE fiber, produced by the gel-spinning process, is 113 GPa [38]. The replacement of toluene with an aliphatic solvent nefras was reflected in the morphology of the UHMWPE reactor powder, namely, in an increase in the number of fibrils (Figure 3b,c), while the degree of crystallinity of these two samples of UHMWPE was determined by DSC and was the same at 55%. The presence of fibrillated elements prevented a uniform distribution of stress in the sample during orientation drawing and, as a result, led to a deterioration in the strength characteristics of film tapes (entries 2 and 3, Table 2). For oriented films from polymers obtained on titanium dichloride complexes **3** and **4**, the maximum values of the average tensile modulus were recorded when using an activator with Et₃Al₂Cl₃.

An important condition for obtaining disentangled UHMWPE is to carry out the polymerization process at low temperatures, which allow to control the rates of polymer chain growth and its crystallization [39]. The fact that many samples obtained at elevated temperatures nevertheless turned out to be suitable for solid-phase processing (Figure 4b, curves 7 and 8) seems very promising to us.

The productivity of systems **1** and 2/Et₃Al₂Cl₃+Bu₂Mg in the ethylene /1-octene copolymerization was noticeably lower than for the homopolymerization of ethylene; i.e., in this case, no positive effect of the comonomer was observed. The molecular weights of the copolymers (1.1–8.9 × 10⁵ Da) were also significantly lower than for the polyethylene

samples (4.8×10^5 – 1.01×10^7 Da) (we can compare these data only at a qualitative level, since different methods of their determination were used).

The percentage of comonomer incorporation was low (1.4–4.6 mol% for precatalyst 1), and it was obvious that an increase in the steric load at the metal center made it difficult for the bulk comonomer, 1-octene, to approach the reaction center. For complex 2, this trend was more pronounced.

The ethylene/1-octene copolymerization process even more clearly demonstrated the increased thermal stability of complexes 1–2: with an increase in the polymerization temperature from 10 to 50 °C, a noticeable increase in productivity was observed, which remains quite acceptable even at a temperature of 70 °C (Figure 5, Table 3). To our surprise, with increasing temperature, the molecular weight of the copolymers increased significantly, reaching a maximum at 50 °C.

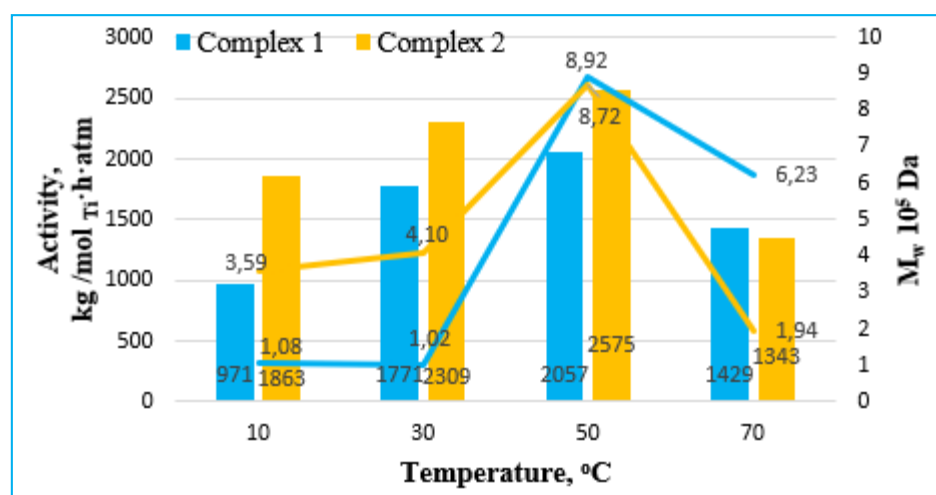


Figure 5. Influence of polymerization temperature on productivity of catalytic systems ethylene/1-octene copolymerization on M_w of resulting copolymers.

Table 3. Ethylene/octene-1 copolymerization ^a.

Entry	Complex	T_p , °C	A, kg/mol·h·atm	Composition (mol %)		T_m (°C)	χ_c (%)	M_w , 10 ⁵ Da	M_w/M_n
				E	O				
1	1	10	971	98.6	1.4	138.2	70.4	1.08	5.37
2	1	30	1771	97.8	2.2	137.5	42.1	1.02	5.53
3	1	50	2057	95.4	4.6	127.7	38.2	8.91	4.23
4	1	70	1429	96.7	3.3	127.5	36.5	6.23	4.88
5	2	10	1863	98.5	1.5	137.1	80.2	3.59	7.98
6	2	30	2309	98.3	1.7	139.7	70.0	4.11	6.31
7	2	50	2575	98.6	1.4	134.2	62.8	8.72	7.69
8	2	70	1343	98.8	1.2	136.1	56.4	1.94	9.36

^a Copolymerization was carried out in 100 mL of toluene with 5×10^{-6} mol of precatalyst at a constant excessive ethylene pressure of 1.7 atm for 30 min; the activator was 1.5 Et₃Al₂Cl₃+Bu₂Mg, and the amount of 1-octene was 10 mL.

4. Conclusions

In summary, new titanium(IV) complexes with OO²⁻-type diolate ligands in the presence of a binary cocatalysts {3Et₂AlCl + Bu₂Mg} or {1.5Et₃Al₂Cl₃ + Bu₂Mg} exhibited moderate to high activities toward ethylene polymerization (460–3260 kg/mol·h·atm). The M_w of the obtained polymer samples reached 10 million Da.

Compared to previously obtained titanium complexes with flexible aliphatic diolate ligands [15–22], complexes 1–4 with a rigid camphane framework were characterized by increased thermal stability. Complex 2 with an increased steric load at hydroxyl groups was able to produce UHMWPE even at a temperature of 70 °C. This UHMWPE sample was processed into an oriented film with a tensile strength of 1.6–2.0 GPa and an average tensile modulus of 108–123 GPa. Films obtained on the same precatalysts at a temperature of 10 °C were characterized by higher values of breaking strength up to 2.7 GPa and modulus up to 151 GPa.

Thus, directed changes in the ligand structure, namely the use of a rigid framework and an increase in the steric load of hydroxyl groups, seem to be a promising direction in the development of thermally stable precatalysts for the polymerization of olefins.

Supplementary Materials: The following supporting information can be downloaded at: <https://www.mdpi.com/article/10.3390/polym14214735/s1>, Figure S1: ^1H NMR spectrum of L2 (400 MHz, CDCl_3); Figure S2: ^1H NMR spectrum of $[\text{L}^1\text{Ti}(\text{OiPr})_2]_2$ (400 MHz, CDCl_3); Figure S3: ^{13}C NMR spectrum of $[\text{L}^1\text{Ti}(\text{OiPr})_2]_2$ (400 MHz, CDCl_3); Figure S4: ^1H NMR spectrum of $[\text{L}^2\text{Ti}(\text{OiPr})_2]_2$ (400 MHz, CDCl_3); Figure S5: ^{13}C NMR spectrum of $[\text{L}^2\text{Ti}(\text{OiPr})_2]_2$ (400 MHz, CDCl_3); Figure S6: ^1H NMR spectrum of L^1TiCl_2 2iPrOH (400 MHz, CDCl_3); Figure S7: ^{13}C NMR spectrum of L^1TiCl_2 2iPrOH (400 MHz, CDCl_3); Figure S8: ^1H NMR spectrum of L^2TiCl_2 2iPrOH (400 MHz, CDCl_3); Figure S9: DSC curves corresponding to UHMWPE produced on 1/ Et_2AlCl + Bu_2Mg (entry 1, Table 1); Figure S10: DSC curves corresponding to UHMWPE produced on 1/ EtAlCl_2 + Bu_2Mg (entry 4, Table 1); Figure S11: DSC curves corresponding to UHMWPE produced on 1/ $\text{Et}_3\text{Al}_2\text{Cl}_3$ + Bu_2Mg , nefras (entry 5, Table 1); Figure S12: DSC curves corresponding to UHMWPE produced on 1/ $\text{Et}_3\text{Al}_2\text{Cl}_3$ + Bu_2Mg , nefras, preactivation (entry 6, Table 1); Figure S13: DSC curves corresponding to UHMWPE produced on 1/ $\text{Et}_3\text{Al}_2\text{Cl}_3$ + Bu_2Mg (entry 8, Table 1); Figure S14: DSC curves corresponding to UHMWPE produced on 1/ $\text{Et}_3\text{Al}_2\text{Cl}_3$ + Bu_2Mg , 70 °C (entry 9, Table 1); Figure S15: DSC curves corresponding to UHMWPE produced on 3/ Et_2AlCl + Bu_2Mg (entry 15, Table 1); Figure S16: DSC curves corresponding to UHMWPE produced on 3/ EtAlCl_2 + Bu_2Mg (entry 17, Table 1); Figure S17: DSC curves corresponding to ethylene/1-octene copolymer produced on 1/ $\text{Et}_3\text{Al}_2\text{Cl}_3$ + Bu_2Mg , 10 °C (entry 1, Table 3); Figure S18: DSC curves corresponding to ethylene/1-octene copolymer produced on 1/ $\text{Et}_3\text{Al}_2\text{Cl}_3$ + Bu_2Mg , 30 °C (entry 2, Table 3); Figure S19: DSC curves corresponding to ethylene/1-octene copolymer produced on 1/ $\text{Et}_3\text{Al}_2\text{Cl}_3$ + Bu_2Mg , 50 °C (entry 3, Table 3); Figure S20: DSC curves corresponding to ethylene/1-octene copolymer produced on 1/ $\text{Et}_3\text{Al}_2\text{Cl}_3$ + Bu_2Mg , 70 °C (entry 4, Table 3); Figure S21: SEM images of the surface morphology of UHMWPE powders obtained with catalytic system 1/ $\text{Et}_3\text{Al}_2\text{Cl}_3$ + Bu_2Mg , entry 8, 50 °C and 3/ $\text{Et}_3\text{Al}_2\text{Cl}_3$ + Bu_2Mg , entry 16, 50 °C; Figure S22: GPC curves corresponding to ethylene/1-octene copolymer produced on 1/ $\text{Et}_3\text{Al}_2\text{Cl}_3$ + Bu_2Mg , 10 °C (entry 1, Table 3); Figure S23: GPC curves corresponding to ethylene/1-octene copolymer produced on 1/ $\text{Et}_3\text{Al}_2\text{Cl}_3$ + Bu_2Mg , 30 °C (entry 2, Table 3); Figure S24: GPC curves corresponding to ethylene/1-octene copolymer produced on 1/ $\text{Et}_3\text{Al}_2\text{Cl}_3$ + Bu_2Mg , 50 °C (entry 3, Table 3); Figure S25: GPC curves corresponding to ethylene/1-octene copolymer produced on 1/ $\text{Et}_3\text{Al}_2\text{Cl}_3$ + Bu_2Mg , 70 °C (entry 4, Table 3); Figure S26: GPC curves corresponding to ethylene/1-octene copolymer produced on 2/ $\text{Et}_3\text{Al}_2\text{Cl}_3$ + Bu_2Mg , 10 °C (entry 5, Table 3); Figure S27: GPC curves corresponding to ethylene/1-octene copolymer produced on 2/ $\text{Et}_3\text{Al}_2\text{Cl}_3$ + Bu_2Mg , 30 °C (entry 6, Table 3); Figure S28: GPC curves corresponding to ethylene/1-octene copolymer produced on 2/ $\text{Et}_3\text{Al}_2\text{Cl}_3$ + Bu_2Mg , 50 °C (entry 7, Table 3); Figure S29: GPC curves corresponding to ethylene/1-octene copolymer produced on 2/ $\text{Et}_3\text{Al}_2\text{Cl}_3$ + Bu_2Mg , 70 °C (entry 8, Table 3). Table S1. Crystal data and structure refinement parameters for 1 and 2. Table S2. Selected geometric parameters and Continuous Symmetry Measures for 1 and 2^a.

Author Contributions: B.M.B.: Funding acquisition, data curation, project administration, and supervision. V.A.T.: Conceptualization, investigation, and writing—review and editing. S.C.G.: investigation, validation, and writing—original draft. D.A.K.: Methodology, investigation, and validation. Y.V.N.: Investigation, formal analysis, and validation. P.V.P.: Investigation. M.D.E.: Investigation. E.K.G.: Methodology, investigation, and formal analysis. M.I.B.: Investigation and formal analysis. G.G.N.: Investigation. P.B.D.: Investigation. V.I.P.: Investigation. K.F.M.: Investigation. All authors have read and agreed to the published version of the manuscript.

Funding: This research was funded by the Russian Science Foundation (Project No. 18-13-00375).

Institutional Review Board Statement: Not applicable.

Informed Consent Statement: Not applicable.

Data Availability Statement: The data presented in this study are available on request from the corresponding author.

Acknowledgments: This work was supported by the Russian Science Foundation (Project No. 18-13-00375). DSC, elemental analysis was performed with the financial support of the Ministry of Science and Higher Education of the Russian Federation employing the equipment of the Center for Molecular Composition Studies of INEOS RAS. X-ray diffraction data were collected using the equipment of the Center for Molecular Composition Studies of INEOS RAS with the financial support from the Ministry of Science and Higher Education of the Russian Federation (Contract/agreement No. 075-00697-22-00). NMR studies of the copolymers were performed with the financial support from the Development Program of the Interdisciplinary Scientific and Educational School of Lomonosov Moscow State University «The future of the planet and global environmental change». The state budget program (project code AAAA-A16-116053110012-5) are also acknowledged with appreciation.

Conflicts of Interest: The authors declare no conflict of interest.

References

1. Valente, A.; Mortreux, A.; Visseaux, M.; Zinck, P. Coordinative Chain Transfer Polymerization. *Chem. Rev.* **2013**, *113*, 3836–3857. [[CrossRef](#)] [[PubMed](#)]
2. Stürzel, M.; Mihan, S.; Mülhaupt, R. From Multisite Polymerization Catalysis to Sustainable Materials and All-Polyolefin Composites. *Chem. Rev.* **2016**, *116*, 1398–1433. [[CrossRef](#)] [[PubMed](#)]
3. Sauter, D.W.; Taoufik, M.; Boisson, C. Polyolefins, a Success Story. *Polymers* **2017**, *9*, 185. [[CrossRef](#)] [[PubMed](#)]
4. Walsh, D.J.; Hyatt, M.G.; Miller, S.A.; Guironnet, D. Recent Trends in Catalytic Polymerizations. *ACS Catal.* **2019**, *9*, 11153–11188. [[CrossRef](#)]
5. Natta, G.; Porri, L.; Carbonaro, A.; Stoppa, G. Polymerization of conjugated diolefins by homogeneous aluminum alkyl-titanium alkoxide catalyst systems. I. *Cis-1,4 isotactic poly (1,3-pentadiene)* *Macromol. Chem.* **1964**, *77*, 114–125. [[CrossRef](#)]
6. Natta, G.; Porri, L.; Carbonaro, A. Polymerization of conjugated diolefins by homogeneous aluminum alkyl-titanium alkoxide catalyst systems. II. 1,2-polybutadiene and 3,4-polyisoprene. *Macromol. Chem.* **1964**, *77*, 126–138. [[CrossRef](#)]
7. Dawes, D.H.; Winkler, C.A. Polymerization of butadiene in the presence of triethylaluminum and n-butyl titanate. *J. Polym. Sci. Part A Polym. Chem.* **1964**, *2*, 3029–3051. [[CrossRef](#)]
8. Al-Sa’doun, A.W. Dimerization of ethylene to butene-1 catalyzed by $Ti(OR')_4-AlR_3$. *Appl. Catal. A* **1993**, *105*, 1–40. [[CrossRef](#)]
9. Gueta-Neyroud, T.; Tumanskii, B.; Kapon, M.; Eisen, M.S. Synthesis and Characterization of Dichlorotitanium Alkoxide Complex and Its Activity in the Polymerization of α -Olefins. *Macromolecules* **2007**, *40*, 5261–5270. [[CrossRef](#)]
10. Suttill, J.A.; McGuinness, D.S.; Pichler, M.; Gardiner, M.G.; Morgan, D.H.; Evans, S.J. Preparation and structures of aryloxy- and alkoxy-Ti(IV) complexes and their evaluation in ethylene oligomerisation and polymerization. *Dalton Trans.* **2012**, *41*, 6625–6633. [[CrossRef](#)] [[PubMed](#)]
11. Hu, H.; Gao, H.; Song, K.; Liu, F.; Long, J.; Zhang, L.; Zhu, F.; Wu, Q. Novel bis(benzoin) titanium catalyst for homo- and copolymerization of norbornene with ethylene: Synthesis, characterization and catalytic properties. *Polymer* **2008**, *49*, 4552–4558. [[CrossRef](#)]
12. Mehta, A.; Tembe, G.; Parikh, P.; Mehta, G. A study of molecular weight regulation in polyethylene by titanium diolate catalysts. *Polym. Int.* **2014**, *63*, 206–213. [[CrossRef](#)]
13. Kissin, Y.V.; Rishina, L.A.; Lalayan, S.S.; Krashennnikov, V.G. A new route to atactic polypropylene: The second life of premetallocene homogeneous polymerization catalyst. *J. Polym. Sci. Part A Polym. Chem.* **2015**, *53*, 2124. [[CrossRef](#)]
14. Rishina, L.A.; Kissin, Y.V.; Lalayan, S.S.; Krashennnikov, V.G.; Perepelitsina, E.O.; Medintseva, T.I. A novel efficient Ti(O-iso-C₃H₇)₄-based olefin polymerization catalyst system. *Polym. Sci. Ser. B* **2016**, *58*, 152–162. [[CrossRef](#)]
15. Tuskaev, V.A.; Gagieva, S.C.; Maleev, V.I.; Borissova, A.O.; Solov’ev, M.V.; Starikova, Z.A.; Bulychev, B.M. Titanium (IV) and zirconium (IV) chloride complexes on the base of chiral tetraaryl-1,3-dioxolane-4,5-dimethanol ligands in the polymerization of ethylene: The promoting role of lithium and magnesium chloride. *Polymer* **2013**, *54*, 4455–4462. [[CrossRef](#)]
16. Gagieva, S.C.; Tuskaev, V.A.; Saracheno, D.; Buyanovskaya, A.G.; Smirnova, O.V.; Zvukova, T.M.; Sizov, A.I.; Bulychev, B.M. Ethylene homopolymerization and copolymerization with 1-hexene and 1-octene catalyzed by titanium(IV) dichloride TADDOLate complex activated with MAO. *Polym. Bull.* **2021**, *78*, 1967–1979. [[CrossRef](#)]
17. Gagieva, S.C.; Tuskaev, V.A.; Fedyanin, I.V.; Buzin, M.I.; Vasil’ev, V.G.; Nikiforova, G.G.; Afanas’ev, E.S.; Zubkevich, S.V.; Kurmaev, D.A.; Kolosov, N.A.; et al. Novel titanium (IV) diolate complexes: Synthesis, structure and catalytic activities in ultra-high molecular weight polyethylene production. *J. Organomet. Chem.* **2017**, *828*, 89–95. [[CrossRef](#)]

18. Tuskaev, V.A.; Gagieva, S.C.; Kurmaev, D.A.; Khrustalev, V.N.; Dorovatovskii, P.V.; Mikhaylik, E.S.; Golubev, E.K.; Buzin, M.I.; Zubkevich, S.V.; Nikiforova, G.G.; et al. Novel titanium (IV) complexes with 1,2-diolate ligands: Synthesis, structure and catalytic activities in ultra-high molecular weight polyethylene production. *J. Organomet. Chem.* **2018**, *877*, 85–91. [CrossRef]
19. Rishina, L.A.; Kissin, Y.V.; Lalayan, S.S.; Gagieva, S.C.; Tuskaev, V.A.; Krashennnikov, V.G.; Grinev, V.G. Polymerization and copolymerization reactions of light alkenes with post-metallocene catalysts containing titanium complexes with bidentate pinacol ligands. *ChemistrySelect* **2020**, *5*, 5763–5770. [CrossRef]
20. Tuskaev, V.A.; Gagieva, S.C.; Lyadov, A.S.; Kurmaev, D.A.; Nikiforova, G.G.; Vasil'ev, V.G.; Zubkevich, S.V.; Saracheno, D.; Sizov, A.I.; Privalov, V.I.; et al. Novel Effective Catalyst Systems Based on Titanium(IV) Alkoxide Complexes for Copolymerization of Ethylene and Hexene-1. *Pet. Chem.* **2020**, *60*, 827–833. [CrossRef]
21. Tuskaev, V.A.; Gagieva, S.C.; Kurmaev, D.A.; Melnikova, E.K.; Zubkevich, S.V.; Buzin, M.I.; Nikiforova, G.G.; Vasil'ev, V.G.; Saracheno, D.; Bogdanov, V.S.; et al. Olefin polymerization behavior of titanium(IV) alkoxo complexes with fluorinated diolate ligands: The impact of the chelate ring size and the nature of organoaluminum compounds. *Appl. Organomet. Chem.* **2020**, *34*, e5933. [CrossRef]
22. Tuskaev, V.A.; Bogdanov, V.S.; Gagieva, S.C.; Kurmaev, D.A.; Shatokhin, S.S.; Evseeva, M.D.; Golubev, E.K.; Buzin, M.I.; Nikiforova, G.G.; Bulychev, B.M. New catalytic systems based on fluorine-containing titanium(IV) alkoxides for the synthesis of ultrahigh-molecular-weight polyethylene and olefin elastomers. *Russ. Chem. Bull.* **2022**, *71*, 76–82. [CrossRef]
23. Tuskaev, V.A.; Gagieva, S.C.; Kurmaev, D.A.; Kolosov, N.A.; Fedyanin, I.V.; Bulychev, B.M. Titanium (IV) complexes stabilized by 2,6-bis-(α,α' -diphenyl(hydroxy)methyl)-pyridine: Catalytic activity in olefin polymerization and impact of lithium and magnesium chlorides. *Inorg. Chim. Acta* **2015**, *425*, 275–281. [CrossRef]
24. Kolosov, N.A.; Tuskaev, V.A.; Gagieva, S.C.; Fedyanin, I.V.; Khrustalev, V.N.; Polyakova, O.V.; Bulychev, B.M. Vanadium (V) and titanium (IV) compounds with 2-[hydroxy(diaryl)methyl]-8-hydroxyquinolines: Synthesis, structure and catalytic behaviors to olefin polymerization. *Eur. Polym. J.* **2017**, *87*, 266–276. [CrossRef]
25. Tuskaev, V.A.; Gagieva, S.C.; Lyadov, A.S.; Kurmaev, D.A.; Zubkevich, S.V.; Shatokhin, S.S.; Simikin, V.E.; Mikhailik, E.S.; Golubev, E.K.; Nikiforova, G.G.; et al. A Titanium(IV) Complex with an OSO-Type Ligand as a Catalyst for the Synthesis of Ultrahigh-Molecular-Weight Polyethylene. *Pet. Chem.* **2020**, *60*, 329–333. [CrossRef]
26. Tuskaev, V.A.; Gagieva, S.C.; Kurmaev, D.A.; Bogdanov, V.S.; Magomedov, K.F.; Mikhaylik, E.S.; Golubev, E.K.; Buzin, M.I.; Nikiforova, G.G.; Vasil'ev, V.G.; et al. Novel titanium(IV) diolate complexes with additional O-donor as precatalyst for the synthesis of ultrahigh molecular weight polyethylene with reduced entanglement density: Influence of polymerization conditions and its implications on mechanical properties. *Appl. Organomet. Chem.* **2021**, *35*, e6256. [CrossRef]
27. Tuskaev, V.A.; Gagieva, S.C.; Churakov, A.V.; Kurmaev, D.A.; Magomedov, K.F.; Evseeva, M.D.; Golubev, E.K.; Buzin, M.I.; Nikiforova, G.G.; Saracheno, D.; et al. Novel Titanium (IV) Diolate Complexes with Thiophene-Containing OSO-type ligand as pre-catalyst for Ethylene polymerization and Ethylene-Propylene copolymerization. *Inorg. Chim. Acta* **2022**, *977*, 122457. [CrossRef]
28. Kissin, Y.V.; Nowlin, T.E.; Mink, R.I.; Brandolini, A.J. A New Cocatalyst for Metallocene Complexes in Olefin Polymerization. *Macromolecules* **2000**, *33*, 4599–4601. [CrossRef]
29. Kissin, Y.V.; Mink, R.I.; Brandolini, A.J.; Nowlin, T.E. $\text{AlR}_2\text{Cl}/\text{MgR}_2$ combinations as universal cocatalysts for Ziegler–Natta, metallocene, and post-metallocene catalysts. *J. Polym. Sci. Part A Polym. Chem.* **2009**, *47*, 3271–3285. [CrossRef]
30. Pyka, I.; Nikl, J.; Schollmeyer, D.; Waldvogel, S.R. The Role of Side-Arms for Supramolecular Affinity Materials Based on 9,9'-Spirobifluorenes. *Eur. J. Org. Chem.* **2017**, *2017*, 3501–3504. [CrossRef]
31. Brisdon, B.J.; England, R.; Mahon, M.F.; Reza, K.; Sainsbury, M. Synthesis of camphor based chiral crown ethers and their interactions with amino acid derivatives. *J. Chem. Soc. Perkin Trans.* **1995**, *2*, 1909–1914. [CrossRef]
32. Dolomanov, O.V.; Bourhis, L.J.; Gildea, R.J.; Howard, J.A.K.; Puschmann, H. OLEX2: A Complete Structure Solution, Re-refinement and Analysis Program. *J. Appl. Cryst.* **2009**, *42*, 339–341. [CrossRef]
33. Sheldrick, G.M. SHELXT—Integrated Space-Group and Crystal-Structure Determination. *Acta Cryst. A* **2015**, *71*, 3–8. [CrossRef] [PubMed]
34. Bourhis, L.J.; Dolomanov, O.V.; Gildea, R.J.; Howard, J.A.K.; Puschmann, H. The anatomy of a comprehensive constrained, restrained refinement program for the modern computing environment—Olex2 dissected. *Acta Cryst.* **2015**, *A71*, 59–75. [CrossRef]
35. Kurtz, M.S. Ultra-high molecular weight polyethylene in total joint replacement. In *The UHMWPE Handbook*; Elsevier Inc.: Amsterdam, The Netherlands, 2004.
36. Ozerin, A.N.; Ivanchev, S.S.; Chvalun, S.N.; Aulov, V.A.; Ivancheva, N.I.; Bakeev, N.F. Properties of oriented film tapes prepared via solid-state processing of a nascent ultrahigh-molecular-weight polyethylene reactor powder synthesized with a postmetallocene catalyst. *Polym. Sci. Ser. A* **2012**, *54*, 950–954. [CrossRef]
37. Alvarez, S. Distortion Pathways of Transition Metal Coordination Polyhedra Induced by Chelating Topology. *Chem. Rev.* **2015**, *115*, 13447–13483. [CrossRef]
38. Available online: https://www.tejinaramid.com/wp-content/uploads/2018/12/18033TEI-Prodbroch-Endumax_LR.pdf (accessed on 5 September 2022).
39. Ronca, S.; Forte, G.; Tjaden, H.; Rastogi, S. Solvent-Free Solid-State-Processed Tapes of Ultrahigh-Molecular-Weight Polyethylene: Influence of Molar Mass and Molar Mass Distribution on the Tensile Properties. *Ind. Eng. Chem. Res.* **2015**, *54*, 7373–7381. [CrossRef]